NASA Technical Memorandum 106546

Numerical Comparison of Convective Heat Transfer Augmentation Devices Used in Cooling Channels of Hypersonic Vehicles

Jaime J. Maldonado
Lewis Research Center
Cleveland, Ohio

April 1994

National Aeronautics and
Space Administration

Numerical Comparison of Convective Heat Transfer Augmentation Devices Used in Cooling Channels of Hypersonic Vehicles

Jaime J. Maldonado
National Aeronautics and Space Administration
Lewis Research Center
Cleveland, Ohio

ABSTRACT

Hypersonic vehicles are exposed to extreme thermal conditions compared to subsonic aircraft; therefore, some level of thermal management is required to protect the materials used. Normally, hypersonic vehicles experience the highest temperatures in the nozzle throat, and aircraft and propulsion system leading edges. Convective heat transfer augmentation techniques can be used in the thermal management system to increase heat transfer of the cooling channels in those areas. The techniques studied in this report are pin-fin, offset-fin, ribbed and straight roughened channel. A smooth straight channel is used as the baseline for comparing the techniques. SINDA '85, a lumped parameter finite difference thermal analyzer, is used to model the channels. Subroutines are added to model the fluid flow assuming steady one-dimensional compressible flow with heat addition and friction. Correlations for convective heat transfer and friction are used in conjunction with the fluid flow analysis mentioned. As expected, the pin-fin arrangement has the highest heat transfer coefficient and the largest pressure drop. All the other devices fall in between the pin-fin and smooth straight channel. The selection of the best heat augmentation method depends on the design requirements. A good approach may be a channel using a combination of the techniques. For instance, several rows of pin-fins may be located at the region of highest heat flux, surrounded by some of the other techniques. Thus, the heat transfer coefficient is maximized at the region of highest heat flux while the pressure drop is not excessive.

INTRODUCTION

There has been an increasing interest in hypersonic vehicles in recent years. Concepts like the National Aerospace Plane (NASP), a single-stage-to-orbit vehicle, and the BETA II, a two-stage-to-orbit vehicle, are being considered as possible replacements for the Space Shuttle. Several hypersonic cruise vehicles are also being studied.

Extreme thermal conditions occur at these high speeds and special care must be taken in areas like the combustor, nozzle, and aircraft and propulsion system leading edges where the worst conditions are normally found. An active cooling system is required to protect the materials from temperatures normally above their melting point.

These cooling systems consist of cooling panels, manifolds, piping, the required turbomachinery, heat exchangers and the coolant. Some designs generate power for the vehicle by expanding the heated coolant in a turbine. Two possible coolants are cryogenic fuels, which remove heat by latent and sensible heat, and endothermic fuels, which remove heat by latent heat, sensible heat and by an endothermic chemical reaction. Para-hydrogen, a cryogenic fuel, is used as the coolant in this study.

Convective heat transfer augmentation techniques, which have been widely used in heat exchangers and turbine blades, can be applied to cooling panels. This paper compares several of these methods: the roughened surface, offset-fin, ribbed and pin-fin channel (Figures 1, 2, 3, and 4, respectively). The methods operate on the principle of increasing the convective heat transfer by increasing the turbulence in the channel. The pin-fin, offset-fin and the ribbed channel have protruding surfaces that disturb the flow. The protruding surfaces of the offset-fin channel form a repetitive staggered fin pattern, which creates a continuously developing flow. The roughened surface increases the turbulence by an increase in the friction. In general, for all these methods, the increase in the convection heat transfer is accompanied by an increased channel complexity and pressure drop.

NOMENCLATURE

A	cross sectional area
Amin	minimum pin-fin channel cross sectional area
$\overline{A}$	average flow area in test section, equation (23)
AR	channel aspect ratio, width / height
c_p	fluid specific heat - constant pressure
D_H	hydraulic diameter, $D_H=4A/\mathcal{P}$
D_P	pin diameter
D'_P	pin characteristic diameter, equation (22)
e	rib height
f_{DW}	Darcy-Weisbach friction factor, $f_{DW}=2\Delta P/(\rho v^2 x/D_H)$
f_F	Fanning friction factor, $f_F=2\Delta P/(4\rho v^2 x/D_H)$
f_P	pin-fin friction factor, $f_P=2\Delta P/(4\rho v^2 N)$
h	heat transfer coefficient
H	channel height
j	Colburn factor, $j=StPr^{2/3}$
k	fluid thermal conductivity
L	length of heated portion of a cell in the flow direction
n	number of rib sharp corners facing the flow
N	number of pin rows
Nu	Nusselt number, $Nu=hD_H/k$
Nu_P	Nusselt number for pin-fin channels, $Nu_P=hD'_P/k$
p	rib pitch
P	pressure
$\mathcal{P}$	wetted perimeter
Pr	Prandtl number, $Pr=c_p\mu/k$
q	dynamic pressure, $q=\rho v^2/2$
r	recovery factor, equation (26)
Re	Reynolds number, $Re=\dot{w}D_H/(A\mu)$
Re_D	Reynolds number for pin-fin channels, $Re_D=\dot{w}D_P/(Amin\ \mu)$
Re_{VF}	Reynolds number defined by VanFossen, equation (21)
S	total heat transfer surface area of a cell
St	Stanton number, $St=h/(\rho v c_p)$
t	offset-fin thickness
T	temperature
TL	total length of the panel
v	fluid velocity, maximum velocity for the case of the pin-fin channel
V	open volume in a cell
$\dot{w}$	mass flow rate
W	channel width
x	axial distance, measured from panel entrance
XL	pin-fin channel spacing, parallel to flow direction
XS	offset-fin length
XT	pin-fin channel spacing, perpendicular to flow direction
α	helix angle of rib
β	contact angle of rib profile
ε	roughness height
ε^*	non-dimensional roughness height, equation (6)
ε/D_H	relative roughness
ρ	fluid density
μ	fluid dynamic viscosity

subscripts:

a	augmented property
aw	adiabatic wall condition
b	bulk condition
in	inlet conditions to the panel
p	pin
r	Eckert reference condition
s	smooth property
st	static condition
t	total condition
w	wall condition

METHOD OF ANALYSIS

A literature search was done on the following convective heat transfer augmentation devices: straight roughened, offset-fin, pin-fin and ribbed channel. A smooth straight channel is selected as the baseline to compare these techniques. Correlations for heat transfer and friction were obtained and are discussed below. The ranges where these correlations can be used are summarized in Tables 1, 2, 3 and 4. Some of these correlations were developed for hydrogen and apply for a Prandtl number close to 0.7.

Straight Channel

i) Smooth Surface

The smooth channel correlations are limited to a relative roughness (ε/D_H) of 10^{-6}. The friction factor for a smooth channel according to the Von-Karman/Nikuradse formula (reference 1), is

$$\frac{1}{\sqrt{f_{DW}}} = -0.8 + 2\log_{10}\left(Re_b\sqrt{f_{DW}}\right) \tag{1}$$

This correlation is evaluated at the bulk temperature and corrected for the wall to bulk temperature difference by

$$\frac{f_{DW}}{f_{DW_b}} = \left[\frac{T_w}{T_b}\right]^{-0.1} \tag{2}$$

This relationship is valid for fully developed turbulent flow of a heated gas in a circular tube and the exponent was obtained by experimentation and analysis (reference 2).

An analytical comparison of heat transfer coefficients for supercritical hydrogen was performed by Dziedzic, et. al. (reference 3). Several correlations developed for hydrogen as the working fluid were compared to the results of a computational fluid dynamics (CFD) code. The following correlation developed by Taylor (reference 4) gave the best agreement with the CFD results, and hence is the one selected for this study.

$$Nu = 0.023\,Re_b^{0.8}\,Pr_b^{0.4}\left[\frac{T_w}{T_b}\right]^{-\left[0.57-1.59\frac{D_H}{x}\right]} \tag{3}$$

All the properties should be evaluated at the fluid bulk temperature and the correlation accounts for entrance effects and difference between the wall and bulk temperatures.

ii) Roughened Surface

The friction factor for a rough channel according to the Colebrook formula (reference 5), is

$$\frac{1}{\sqrt{f_{DW}}} = \log_{10}\left[\frac{\varepsilon}{3.7D_H} + \frac{2.51}{Re_b\sqrt{f_{DW}}}\right]^{-2} \tag{4}$$

The correlation is evaluated at the bulk temperature and the correction for the wall and the bulk temperature difference is made using equation 2.

The roughness effects on heat transfer are evaluated using a heat transfer similarity law developed by Dipprey and Sabersky (reference 6). The flow can be divided into three regions: smooth, transition and fully rough, and each one can be characterized by a different range of roughness values. Using the non-dimensional roughness height to describe these regions, they can be arranged as follows:

$\varepsilon^* < 3.32$	Smooth
$3.32 \leq \varepsilon^* \leq 67.0$	Transition
$\varepsilon^* > 67.0$	Fully rough

The heat transfer similarity law obtained is

$$\frac{f_{DW}/(8\,St) - 1}{\sqrt{f_{DW}/8}} + 8.48 = g(\varepsilon^*, Pr) \tag{5}$$

where:

$$\varepsilon^* = Re(\varepsilon/D_H)\sqrt{f_{DW}/8} \tag{6}$$

and

$$g(\varepsilon^*, Pr) = 6.7\,Pr^{0.44} \quad \text{Smooth} \tag{7}$$

$$g(\varepsilon^*, Pr) = 5.30\,\varepsilon^{*0.195}\,Pr^{0.44} \quad \text{Transition} \tag{8}$$

$$g(\varepsilon^*, Pr) = 5.19\,\varepsilon^{*0.2}\,Pr^{0.44} \quad \text{Fully rough} \tag{9}$$

These g-functions apply to granular close-packed roughness, used by Dipprey and Sabersky in their experiment. This sand grain roughness is three-dimensional and is qualitatively similar to the tube surface. For the smooth and transition regions, the g-functions only apply to a Prandtl number near 0.7.

A mathematical procedure using the heat transfer similarity law (equations 5 to 9) is used to evaluate the improvement in the heat transfer due to the roughness. First, the smooth region heat transfer is calculated using the heat transfer similarity law with the friction factor from equation 1, while the transition or the fully rough region heat transfer is calculated with the friction factor from equation 4. Second, a ratio of the previously obtained heat transfer coefficients between the roughened and smooth regions is obtained. Finally, the ratio is multiplied to the result of the correlation proposed by Taylor (equation 3), resulting in the estimated roughened heat transfer. This procedure besides evaluating the roughness effect on heat transfer also accounts for entrance and temperature effects, which are not considered in the heat transfer similarity law.

Offset-fin Channel

This type of channel has fins offset by half of the channel width, preventing the flow from reaching a fully developed behavior. This continuously developing flow inherits the higher heat transfer characteristics of the entry region of the straight channel. The friction and heat transfer correlations developed by Wieting (reference 7) for an offset-fin channel were selected for this study:

$$f_F = 1.136\left[\frac{XS}{D_H}\right]^{-0.781}\left[\frac{t}{D_H}\right]^{0.534} Re_b^{-0.198} \tag{10}$$

$$j = 0.242\left[\frac{XS}{D_H}\right]^{-0.322}\left[\frac{t}{D_H}\right]^{0.089} Re_b^{-0.368} \tag{11}$$

The heat transfer and pressure loss are independent of aspect ratio over the range studied by Wieting, but for extreme values of aspect ratios it will make a difference. This correlation should be used only for gaseous cooling fluids with Prandtl numbers near 0.7. Since there is a lack of information for this type of heat transfer augmentation device, further studies and tests are recommended in this area to corroborate the results obtained by Wieting and expand the region where this correlation can be used.

The temperature effects are very small for this type of heat transfer augmentation device. Kays and London (reference 2) recommend that all properties should be evaluated at the bulk temperature and no correction for wall to bulk temperature difference be used for all the interrupted-boundary-layer surfaces.

Ribbed Channel

For the ribbed channel the friction and heat transfer correlations developed by Ravigururajan and Bergles (reference 8) are used. The correlations, developed from a statistical analysis done on test data of previous investigations, apply to a wide range of geometric and flow parameters. The set of correlations yields better results than similar approaches to the same problem carried out by other researchers. The correlations provide a correction factor for the increased pressure drop and heat transfer over that of the smooth straight channel:

$$\frac{f_{F_a}}{f_{F_s}} = \left\{1+\left[29.1 Re_b^{\left(0.67-0.06\frac{p}{D_H}-0.49\frac{\alpha}{90}\right)}\cdot\left(\frac{e}{D_H}\right)^{\left(1.37-0.157\frac{p}{D_H}\right)}\cdot\left(1+\frac{2.94}{n}\right)\sin\beta\right.\right.$$
$$\left.\left.\cdot\left(\frac{\alpha}{90}\right)^{\left(4.59+4.11\times10^{-6}Re_b-0.15\frac{p}{D_H}\right)}\cdot\left(\frac{p}{D_H}\right)^{\left(-1.66\times10^{-6}Re_b-0.33\frac{\alpha}{90}\right)}\right]^{15/16}\right\}^{16/15} \tag{12}$$

$$\frac{Nu_a}{Nu_s} = \left\{1+\left[2.64 Re_b^{0.036}\cdot\left(\frac{e}{D_H}\right)^{0.212}\cdot\left(\frac{p}{D_H}\right)^{-0.21}\cdot\left(\frac{\alpha}{90}\right)^{0.29} Pr_b^{-0.024}\right]^7\right\}^{1/7} \tag{13}$$

where:

n = 2, for triangular and rectangular rib profiles

n = ∞, for any curved rib profile

β = 90°, for any curved rib profile (Figure 3)

These correlations apply for a single phase fluid in turbulent flow. Different types of rib profiles can be studied, but a change of the rib profile only influences the pressure losses, since it does not have any effect on the heat transfer in the correlations used.

Ravigururajan and Bergles used the Filenenko (reference 9) straight smooth tube friction factor correlation and the Petukhov and Popov (reference 10) straight smooth tube heat transfer correlation to develop their ribbed channel correlations. The smooth straight channel correlations are

$$f_{F_s} = \left[1.58\ln(Re_b) - 3.28\right]^{-2} \tag{14}$$

$$Nu_s = \frac{\left(f_{F_s}/2\right) Re_b \, Pr_b}{1.07 + 12.7\sqrt{f_{F_s}/2}\left(Pr_b^{2/3} - 1\right)} \tag{15}$$

These straight smooth tube correlations were compared to the correlations previously discussed (equations 1 and 3) and a graphical representation can be found in Figures 5 and 6. Equation 15 has a better agreement with equation 3 when corrected for the wall to bulk temperature difference. The previously discussed wall to bulk temperature difference correction for the friction factor correlation (equation 2) and a similar correction for the heat transfer correlation are used with equations 14 and 15. The correction for heat transfer correlation is

$$\frac{Nu}{Nu_b} = \left[\frac{T_w}{T_b}\right]^{-0.5} \tag{16}$$

This relationship was developed under the same conditions as equation 2 (reference 2). The correlations by Filenenko and by Petukhov and Popov along with the wall to bulk temperature corrections were selected to be used in conjunction with the correlation for the ribbed channel. The ribbed channel correlations are tailored for the Filenenko friction factor correlation and the Petukhov and Popov heat transfer correlation; therefore, a more accurate prediction is believed to be obtained with these correlations. Including the thermal effects through equations 2 and 16 yields a better prediction of friction and heat transfer, since this effect was not originally considered in the correlations by Ravigururajan and Bergles.

Pin-fin Channel

Pin-fin arrays can be divided into two types; short pins, normally used in internal passages of turbine blades, and long pins, common in heat exchangers. Long pin arrays have a height ratio (height over pin diameter) larger than eight, and the heat transfer on the pin surface is dominant. Those with height ratios of less than four are considered short pin arrays, and the end wall heat transfer is dominant. Although the use of short pin-fins can reduce the total heat transfer surface area, they still increase the total heat transfer over a channel with no pins by increasing the level of turbulence in the flow.

The average heat transfer for short pins is less than for long pins due to the end wall effects near the pin. These effects can be observed one diameter away from the end wall. Pin-fin channels show a small developing entrance region of about three to four rows where the heat transfer increases rapidly and then remains nearly constant.

A great number of friction factor and heat transfer correlations have been developed for pin-fins. After comparing several correlations with available data, Armstrong and Winstanley (reference 11) recommended the Metzger friction factor correlation and the VanFossen or Metzger heat transfer correlations. A friction factor correlation developed by Damerow applies for a larger pin spacing, complementing the correlation by Metzger and increasing the range where the friction factor can be calculated. This study uses the friction factor correlation by Metzger for the small spacing and Damerow for the large spacing and the heat transfer correlation by VanFossen. The Metzger friction factor correlation (reference 12) is

$$f_P = 0.317 Re_{Db}^{-0.132} \tag{17}$$
$$\text{for} \quad 10^3 \le Re_{Db} \le 10^4$$

and

$$f_P = 1.76 Re_{Db}^{-0.318} \tag{18}$$
$$\text{for} \quad 10^4 \le Re_{Db} \le 10^5$$

The Damerow friction factor correlation (reference 13) is

$$f_P = 2.06\left(\frac{XT}{D_H}\right)^{-1.1} Re_{D_b}{}^{-0.16} \tag{19}$$

The friction factor is not affected by the wall to bulk temperature difference (reference 2).

The VanFossen heat transfer correlation (reference 14) is

$$Nu_P = 0.153 Re_{VF}{}^{0.685} \tag{20}$$

where:

$$Re_{VF} = \frac{(\dot{w}/\overline{A})D'_P}{\mu} \tag{21}$$

$$D'_P = \frac{4V}{S} \tag{22}$$

$$\overline{A} = \frac{V}{L} \tag{23}$$

VanFossen recommends all the properties be evaluated at the Eckert reference temperature;

$$T_r = 0.5T_w + 0.28T_{st} + 0.22T_{aw} \tag{24}$$

where:

$$T_{aw} = T_{st} + r(T_t - T_{st}) \tag{25}$$

$$r = \sqrt{Pr} \tag{26}$$

VanFossen also demonstrated that the heat transfer on the pin surface is 35% higher than the heat transfer on the end walls and this is accounted for in this study.

Computer Code

A computer model using SINDA '85 (reference 15) was developed to simulate the behavior of these cooling channels and evaluate all the important properties of the coolant and the channels. SINDA '85 is a lumped parameter finite difference computer program that computes temperature and energy balances. It allows the user to write FORTRAN subroutines and pass the desired information to the main program with access to all important variables. SINDA '85 divides a model into nodes and conductors; nodes are network elements that describe how energy is stored during transient analyses; conductors are network elements that describe how energy is transported between nodes. The model obtains all the coolant properties from GASPLUS (reference 16), a computer program that provides the thermodynamic and transport properties of many fluids and fluid mixtures over a wide range of temperatures and pressures. The original version of GASPLUS uses FORTRAN function calls to evaluate fluid properties. This version was modified to use subroutine calls and was assembled by Petley, et. al. (reference 17) due to internal file conflicts with SINDA '85.

The cooling channels are first divided into small cells consisting of only one elemental fin; for instance, one pin and the flow volume around it form a cell. The necessary number of cells is connected to obtain the desired cooling channel length. Each cell is divided into nodes and conductors, then arranged to provide a reasonably accurate temperature prediction balanced by moderate computer execution times. The trade-off between model accuracy and execution time was facilitated by using the commercial finite element model generation software PATRAN (reference 18) and the commercial finite element software MARC (reference 19). A very fine and computer intensive MARC finite element model is used as a baseline, and the SINDA '85 mesh density is compared to this baseline layout. This mesh refinement process is repeated until the SINDA '85 mesh gives an acceptable prediction and still keeps the computer execution time a minimum. The arrangement for all the rectangular cross sectional models was obtained from previous work done by Petley et al. (reference 17).

FLUINT, the SINDA '85 hydraulic computation module, was not used for the model because it assumes incompressible flow, and model generation is more difficult. The fluid flow analysis is performed by a

subroutine based on steady one-dimensional compressible ideal gas flow with heat addition and friction. The fluid flow subroutine accounts for contraction and expansion effects found at the entrance and exit of a channel (reference 5). These effects were included for the straight and ribbed channel models. The offset-fin and pin-fin models take into account these effects in their friction factor correlations. The concept of the hydraulic diameter is used to account for the effects of non-circular cross sections, and for pin-fin channels the hydraulic diameter is evaluated at the minimum cross sectional area.

The thermal conductance for the convective and conductive conductors is evaluated in subroutines developed for each type of channel cross section. A two-dimensional heat conduction model is used for all the channels. The computer model does not account for axial conduction in the channel because the heat transfer in this direction is appreciably lower than the heat transfer through the cross section for the geometries and heat fluxes of interest. Advection heat transfer, energy transport due to bulk fluid motion, is accounted for in the computer model.

The computer model has several features that make it user-friendly without sacrificing any required capability. Most of the important variables are input to the computer model via a NAMELIST input file. This allows the user to model any desired geometry and conditions easily. Properties like the heat flux and the panel material conductivity are input directly to SINDA '85 arrays. A singlet array is dedicated to the heat flux, and one value of heat flux is required for each cell. The model generation is a simple task since most of the related computations during this stage are automated, solving the problem of cumbersome model generation associated with SINDA '85. The computer model creates its own output file along with the SINDA '85 output file.

Since each cell has three walls (top, bottom and side), the wall temperature is evaluated at each cell by averaging these three wall temperatures and weighting them according to their surface areas. This is consistent with the assumption of a one-dimensional fluid flow model. Within one cell, only one value of film coefficient is calculated and applied to the top, side and bottom walls. The pin-fin channel is the only exception, since the film coefficient on the pin surface is 35% higher than the value at the top and bottom wall, following the observation by VanFossen (reference 14).

RESULTS AND DISCUSSION

To understand the behavior and performance of the heat augmentation devices four studies were performed. First, a parametric study of the significant variables for each of the heat augmentation methods was performed to assess the importance of the parameters on the channel performance. Second, a coolant thermodynamic and transport property study was performed for para-hydrogen, in which the temperature and pressure effects and the Reynolds and Prandtl number variation were investigated. Third, a comparative study using similar geometry was accomplished to demonstrate how the methods performed under the same conditions. This allowed for a more direct comparison between methods. During this study the coolant flow area and other important geometric parameters like channel wall thickness were maintained the same between methods (Table 5). Fourth, an optimized geometry comparison study was performed in which design criteria were specified and the geometry varied until the channel with the minimum coolant mass flow rate was obtained (Table 6). Cooling panel thermal stresses, weights and life prediction, although important in the cooling panel design, were not addressed in this study. Throughout all these studies a smooth straight channel was used as the baseline for comparing the different heat augmentation techniques, and para-hydrogen was used as the coolant.

Study i: Parametric

The main goal of this study was to obtain a qualitative understanding of the impact of important parameters on the cooling panel performance. Some of the work done previously on these cooling techniques by other researchers includes quantitative results of similar parametric studies (references 8, 11, 12, 13).

While keeping the Reynolds number constant, changes in the geometry of the straight channel do not have an appreciable effect in the convection heat transfer performance, but even though the convection is not affected, the conduction heat transfer could be heavily influenced by these changes. It is desirable to prolong the entrance effects as long as possible because this increases the heat transfer substantially. Roughness, as expected, increased the heat transfer and the pressure losses, for some cases dramatically.

As the roughness is increased, the flow goes from smooth to transitional to fully rough. The major change occurs in the transition region, and once in the fully rough region the benefits of increasing the roughness are less significant because the pressure drop increases rapidly.

The offset-fin channel has two main factors that affect the performance: increasing the fin thickness increases the heat transfer and the pressure loss, and increasing the fin length decreases the heat transfer and the pressure loss. These effects are more pronounced at the smaller values of fin length and thickness.

The rib pitch and height were the parameters studied for the ribbed channel. As the rib height increases the pressure loss and the heat transfer increase. The heat transfer change is more pronounced at the smaller values; conversely, the change in pressure loss is more pronounced at the larger values. As the rib pitch increases the pressure loss and the heat transfer decrease, and is more pronounced at the smaller pitches.

Only the pin spacing was studied for the pin-fin channel because for a constant Reynolds number a change of the pin height does not substantially affect the performance of the short pin arrays (reference 11). The pins were arranged in an equilateral triangular spacing, making the distance between two pins the same regardless of the direction. Hence the pin spacing varies proportionally in the directions parallel and perpendicular to the flow. An increase of the pin spacing always decreases the heat transfer for the pin-fin geometries in Table 4. This effect does not affect the pressure loss for a small pin spacing (equations 17 and 18), while it decreases the pressure loss for a large pin spacing (equation 19).

Study ii: Coolant properties

The hydrogen coolant properties were studied for a temperature range from 100 to 1200 °R and a pressure range from 900 to 1000 psia (Figures 7 and 8). All properties show drastic changes between 100 and 200 °R, while above this value the changes are linear. For the total temperature range there is a substantial property change. The effect of the pressure, on the other hand, causes small linear changes throughout the range.

For constant geometry and constant coolant mass flow rate, the variation of the Reynolds number and the Prandtl number is only a function of the coolant thermodynamic and transport properties. The representative Reynolds number and Prandtl number for the comparative study using similar geometry (Study iii), based on the bulk temperature and hydraulic diameter, are presented in Figure 9. The coolant temperature in this study increases from 100 to almost 500 °R, hence the location inside the cooling channel can be correlated to the coolant temperature. A good understanding of these non-dimensional parameters gives insight into how the heat transfer and the pressure loss behave in the cooling channel. A drastic variation at the entrance of the cooling channel up to x/TL=0.2 can be observed. Although this appears similar to an entrance effect, it is actually due to the large change in thermodynamic and transport properties at the low temperatures. The constant value of the Prandtl number along most of the channel shows the linear change of the properties for temperatures above 200 °R.

Study iii: Comparison with similar geometry

The Nusselt numbers for the heat transfer augmentation techniques are compared in Figure 10. The entrance effects in the straight channel can be easily observed and the increment on the heat transfer can be as large as two times the fully developed value. The rest of the increment comes from the large variation of the properties at low temperatures. The Nusselt number remains nearly constant through the rest of the channel because the decrease in the Reynolds number is balanced by the decreasing wall to bulk temperature ratio. It can also be seen that the increase in heat transfer due to the increased roughness in a channel diminishes. The Nusselt number for the ribbed channel increases for the first half of the channel and then decreases through the second half. This is due to the rapid change of the coolant properties at low temperatures, the reduction of the Reynolds number and the reduction of the wall to bulk temperature ratio. First, the coolant property variations outpace the other two effects and the heat transfer increases, but as the coolant properties become more stable the other effects dominate and the heat transfer decreases. The Nusselt number for the offset-fin channel remains almost constant near the channel entrance but then decreases throughout the rest of the channel, very similar to the behavior of the Reynolds number. The pin-fin channel shows a similar behavior to the offset-fin channel, with the main

difference near the entrance of the channel. The coolant properties for the pin-fin channel are evaluated at the Eckert reference temperature, which is higher than the bulk temperature; therefore, most of the drastic fluctuation of the properties at the low temperatures is not experienced. A more accurate temperature effects model for hydrogen coolant at low temperatures might be obtained by using equation 16 rather than the Eckert reference temperature, since equation 16 considers the temperature range of drastic fluctuations when evaluating the temperature effects. This will have to be verified with additional work.

The film coefficient curves (Figure 11) are very similar to the Nusselt number curves (Figure 10), because the only difference between them is the effect of the hydrogen thermal conductivity. The drastic change in thermal conductivity at the low temperatures explains the rapid increase in film coefficient found following the entrance (after x/TL=0.2) for the first half of all the cooling channel configurations except the pin-fin channel. The film coefficient for the pin-fin channel does not increase as fast as the others, because the conductivity is evaluated at a reference temperature above this area of highest change in thermal conductivity. The increase in the film coefficient is the highest for the ribbed channel because the variation of the wall to bulk temperature is the largest.

The pressure coefficient for all the heat augmentation methods is presented in Figure 12. The offset-fin channel has the highest pressure loss of all the heat augmentation methods because this method has the largest surface area and the sharpest flow area reduction (53%). The offset-fin thickness has the same dimension as the pin diameter since the goal in this study was to evaluate the methods under the same geometric basis (Table 5). The ribbed channel has the same amount of surface area as the offset-fin channel, but the area reduction due to the ribs is smaller (13%). The pin-fin channel has an area reduction larger than the ribbed channel (35%) but the area transition is the smoothest of all the heat augmentation methods studied and it also has the minimum surface area. By contrast the straight channel only experiences a pressure loss due to the contact with the surface and heat transfer.

The total augmentation factor (Figure 13) is defined here as the ratio of Nusselt number to pressure coefficient normalized by this same ratio for the straight smooth channel. The total augmentation factor and the Goodness Factor, which is the ratio of the Colburn factor to the friction factor should not be confused; although, both are ratios of non-dimensional heat transfer to non-dimensional pressure loss. These factors are indicators of the degree of the efficiency in which the heat transfer augmentation is performed. All the heat augmentation methods studied show an increase to a maximum value near x/TL=0.2 due to the large value of the Nusselt number for the straight smooth channel within the entrance region. The straight roughened channels have a total augmentation factor greater than one, indicating an increase of the heat transfer higher than the increase of the pressure loss. The pin-fin channel has the largest value of total augmentation factor and for the first half of the cooling channel a value higher than the value for the straight roughened channels; thereafter, the straight roughened channels have larger values.

Study iv: Optimized geometry

A typical cooling channel design criteria (Table 6) with no cooling panel weight, stresses nor life prediction considerations was specified for this part of the study and all heat augmentation methods were subjected to these constraints. The model was considered to be optimized when all the aforementioned constraints were fulfilled and the coolant mass flow rate was a minimum. The optimized channel geometry for all the heat augmentation methods is presented in Table 7.

The Nusselt number, film coefficient, pressure coefficient and total augmentation factor are presented in Figures 14, 15, 16 and 17 respectively, and the behavior of the heat augmentation methods is consistent with the previous study. Comparing the results of studies iii and iv one can observe, due to the different channel geometry, the reduction of the Nusselt number and film coefficient for the offset-fin channel and the increase of the pressure loss for the ribbed channel. The difference between the film coefficient for the pin-fin channel and the other heat augmentation methods in this study is larger than the difference for the Nusselt number, because the calculation of the film coefficient involves the evaluation of the thermal conductivity, which is higher for the pin-fin channel due to the higher coolant temperature (Figure 19). In general, the total augmentation factor is smaller for this study than for the previous study indicating that the trade-off between heat transfer and pressure loss is not optimum when the mass flow rate is minimized. For the straight roughened channels of this study, the 180×10^{-6} inches roughness shows a

higher total heat augmentation factor, contrary to the observation in the previous study. The pressure loss increases more between different roughness values in this study than in the previous study while the Nusselt number increases less, leading to a reduction of the total augmentation factor as the roughness increases.

The pin-fin channel required the least mass flow rate (33% lower than for the smooth straight channel) while the smooth straight channel required the most mass flow rate (Figure 18). The straight roughened channels studied required about the same amount of mass flow rate. The mass flow rates required for the offset-fin and ribbed channels are nearly the same, although somewhat less than what the straight roughened channels required. One can also observe that the benefit of roughness on heat transfer decreases as the roughness of the channel is increased. Increasing the roughness to 180×10^{-6} inches from the smooth channel reduced the mass flow rate by (10%), while increasing the roughness to 300×10^{-6} inches reduced the mass flow rate about 2% from the 180×10^{-6} inches (12% from the smooth channel).

The coolant exit temperatures (Figure 19) are consistent with the mass flow rates. The total energy applied to each one of the heat augmentation devices is the same; therefore, a reduction of the mass flow rate is reflected in an increase of the exit coolant temperature.

The straight roughened channels, the offset-fin channel and the ribbed channel still have potential of reducing the coolant mass flow even further, because the pressure drop is less than 100 psia (Table 6, Figure 20). This is mainly because the channel dimensions were limited to values that could be easily manufactured instead of any arbitrary value. A change in any of the leading parameters of these heat augmentation techniques will increase the heat transfer and the pressure drop, reducing the required coolant mass flow rate. The relative order of the coolant exit pressure for some of the heat augmentation devices does not agree with the pressure coefficient (Figure 16) due to the different coolant mass flow rate and channel geometry that each heat augmentation method has. This leads to different velocities inside the cooling channels, which results in different inlet dynamic pressures for each channel.

CONCLUDING REMARKS

It is clearly shown that heat transfer augmentation devices should only be used in circumstances that truly require the higher heat transfer coefficient and where the larger pressure drop can be tolerated. The correlations presented can be used to obtain a first order estimate of the performance of channels using such devices. Geometry plays an important role in the behavior of the heat augmentation devices; therefore, it is not advisable to use these correlations outside the range for which they were developed because this could lead to inaccurate results. Of all the methods studied, the pin-fin yields the highest heat transfer increase accompanied by the highest pressure drop. Pin-fin channels are the best heat augmentation technique for applications where the temperature constraints are more critical than the pressure constraints, for instance leading edges and nozzle throat of hypersonic vehicles. The straight roughened channels have the best trade-off between pressure drop and heat transfer increase. When the pressure constraints are more critical than the temperature constraints, the best heat augmentation method is a straight roughened channel, perhaps the inlet of a hypersonic vehicle. A cooling panel can be tailored to the specific applications to maximize the heat transfer and minimize the pressure loss. The heat augmentation methods with the higher heat transfer can be used in the areas where the heat flux reaches a maximum, while the other methods can be used where the heat flux is lower to minimize the pressure loss.

ACKNOWLEDGMENTS

The author wants to thank Theodore T. Mockler for all the valuable information and help throughout this study.

REFERENCES

1. Saad, M.A.; "Compressible Fluid Flow", Prentice-Hall, 1985.

2. Kays, W.M.; London, A.L.; "Compact Heat Exchangers (2nd Edn.)", Chap. 4, McGraw-Hill 1964.

3. Dziedzic, W.M.; Jones, S.C.; Gould, D.C.; Petley, D.H.; "An Analytical Comparison of Convective Heat Transfer Correlations in Supercritical Hydrogen", AIAA Paper 91-1382, Thermophysics Conference, June 1991.

4. Taylor, M.F.; "Correlation of Local Heat-Transfer Coefficients for Single-Phase Turbulent Flow of Hydrogen in Tubes with Temperature Ratios to 23", NASA-TN-D-4332, 1968.

5. Hodge, B.K.; "Analysis and Design of Energy Systems", Chap. 1, Prentice-Hall, 1985.

6. Dipprey, D.F.; Sabersky, R.H.; "Heat and Momentum Transfer in Smooth and Rough Tubes at various Prandtl Numbers", International Journal of Heat and Mass Transfer, Vol. 6, pp. 329-353, Pergamom Press 1963.

7. Wieting, A.R.; "Empirical Correlations for Heat Transfer and Flow Friction Characteristics of Rectangular Offset-Fin Plate-Fin Heat Exchangers", Journal of Heat Transfer, Transactions of ASME, pp. 488-490, August 1975.

8. Ravigururajan, T.S.; Bergles, A.E.; "General Correlations for Pressure Drop and Heat Transfer for Single-Phase Turbulent Flow in Internally Ribbed Tubes", Augmentation of Heat Transfer in Energy Systems, Transactions of ASME, pp. 9-20, HTD-Vol. 52, November, 1985.

9. Webb, R.L.; "A Critical Evaluation of Analytical Solutions and Reynolds Analogy Equations for Turbulent Heat and Mass Transfer in Smooth Tubes", Waerme-und Stoffubertragung, Vol. 4, 1971, pp. 197-204.

10. Petukhov, B.S.; Popov, V.N.; "Theoretical Calculation of Heat Exchange and Frictional Resistance in Turbulent Flow in Tubes of an Incompressible Fluid with Variable Physical Properties", High Temperature, Vol. 1, pp. 69-83, 1963.

11. Armstrong, J.; Winstanley, D.; "A Review of Staggered Array Pin Fin Heat Transfer for Turbine Cooling Applications", Journal of Turbomachinery, Transactions of ASME, Vol. 110, pp. 94-103, January 1988.

12. Metzger, D.E.; Fan, Z.X.; Shepard, W.B.; "Pressure Loss and Heat Transfer Through Multiple Rows of Short Pin Fins", Heat Transfer 1982, Vol. 3, pp. 137-142, U. Grigull et al., eds., Hemisphere, Washington.

13. Damerow, W.P.; Murtaugh, J.P.; Burggraf, F.; "Experimental and Analytical Investigation of the Coolant Flow Characteristics in Cooled Turbine Airfoils", NASA CR-120883.

14. VanFossen, G.J.; "Heat Transfer Coefficients for Staggered Array of Short Pin Fins", NASA Technical Memorandum 81596, 1981.

15. Cullimore, B.A.; Goble, R.G.; Jensen, C.L.; Ring, S.G.; "SINDA '85/FLUINT User's Manual", Denver Aerospace Division of Martin Marietta Corp., Denver Colorado, March 1990.

16. Fowler, J.R.; "GASPLUS User's Manual (Preliminary NASP Copy)", NASA Lewis Research Center, August 1988.

17. Petley, D.; Jones, S.; Dziedzic, W.; "Analysis of Coolant Systems for Hypersonic Aircraft", AIAA Paper 91-5063, International Aerospace Plane Conference, December 1991.

18. Anon.; "PATRAN Plus User's Manual", Patran division of PDA Engineering, September 1989.

19. Anon.; "MARC User's Manual", Vol. A, B and C, MARC Analysis Research Corporation, January 1990.

20. Yeh F.C.; Stepka, F.S.; "Review and Status of Heat-Transfer Technology for Internal Passages of Air-Cooled Turbine Blades", NASA Technical Paper 2232, 1984.

21. Rohsenow, W.M.; Hartnett, J.P.; Ganic, E.N.; "Handbook of Heat Transfer Applications (2nd Edn.)", Chap. 4, pp. 221-240, McGraw-Hill, 1985.

x/D_H	2 - 252
T_w/T_b	1.1 - 23
Re_b	7500 - 13.8 x 10^6
T_w (°R)	114 - 5630
Heat Flux (BTU/sec in^2)	0.036 - 27.6

Table 1. Summary of ranges for straight channel, heat transfer correlation.

AR	0.162 - 1.196
XS/D_H	0.7 - 5.6
t/D_H	0.030 - 0.166
Re_b	2000 - 50000

Table 2. Summary of ranges for offset-fin channel, friction and heat transfer correlations.

e/D_H	0.01 - 0.2
p/D_H	0.1 - 7.0
$\alpha/90°$	0.3 - 1.0
Re_b	5000 - 250000
Pr_b	0.66 - 37.6

Table 3. Summary of ranges for ribbed channel, friction and heat transfer correlations.

	Heat Transfer VanFossen	Friction Factor Metzger	Friction Factor Damerow
H/D_p	0.5 - 2.0	0.5 - 6.0	2.0 - 4.0
XT/D_p	2.0 - 4.0	1.05 - 5.0	2.12 - 3.54
XL/D_p		2.0 - 4.0	4.24 - 7.07
Re_{VF}	300 - 60000		
Re_{D_b}		1000 - 100000	100 - 40000

Table 4. Summary of ranges for pin-fin channel, friction and heat transfer correlations.

	Straight channel	Offset-fin channel	Ribbed channel	Pin-fin channel
Channel mass flow rate, $\dot{w}$ ($\times 10^5$ lbm/sec)	200.0	200.0	200.0	200.0
Total channel length, TL (in)	5.000	5.000	5.000	5.000
Hydraulic diameter, D_H (in)	0.060	0.060	0.060	0.060
Channel top and bottom wall thickness (in)	0.025	0.025	0.025	0.025
Channel side wall thickness (in)	0.040	0.040	0.040	
Channel height, H (in)	0.050	0.050	0.050	
Channel width, W (in)	0.0755	0.0755	0.0755	
Cell length, L (in)	0.100			
Fin length, XS (in)		0.100		
Rib height, e (in)			0.002	
Rib pitch, p (in)			0.100	
Pin diameter, D_P (in)				0.040
Pin height, H (in)				0.050
Perpendicular to flow pin spacing, XT (in)				0.1155
Parallel to flow pin spacing, XL (in)				0.100

Table 5. Geometry for study comparing channels with similar geometry (study iii).

Uniform heat flux	720 BTU/ft^2 sec
Area to be cooled (length × width)	1 × 2 (ft × ft)
Coolant inlet temperature	100 °R
Panel inlet pressure	1000 psia
Maximum pressure drop	100 psia
Maximum panel temperature	1800 °R
Coolant	Para-hydrogen
Panel Material	Haynes 188
Avoid thermal choking at panel exit	
Minimize the coolant mass flow rate	

Table 6. Cooling panel design criteria (study iv).

	Straight channel	Offset-fin channel	Ribbed channel	Pin-fin channel
Hydraulic diameter, D_H (in)	0.044	0.037	0.044	0.034
Channel top and bottom wall thickness (in)	0.025	0.025	0.025	0.025
Channel side wall thickness (in)	0.025	0.006	0.025	
Channel height, H (in)	0.040	0.040	0.040	
Channel width, W (in)	0.050	0.034	0.050	
Cell length, L (in)	0.100			
Fin length, XS (in)		0.040		
Rib height, e (in)			0.005	
Rib pitch, p (in)			0.150	
Pin diameter, D_P (in)				0.040
Pin height, H (in)				0.020
Perpendicular to flow pin spacing, XT (in)				0.161
Parallel to flow pin spacing, XL (in)				0.140

Table 7. Cooling channel geometry for study of optimized geometry (study iv).

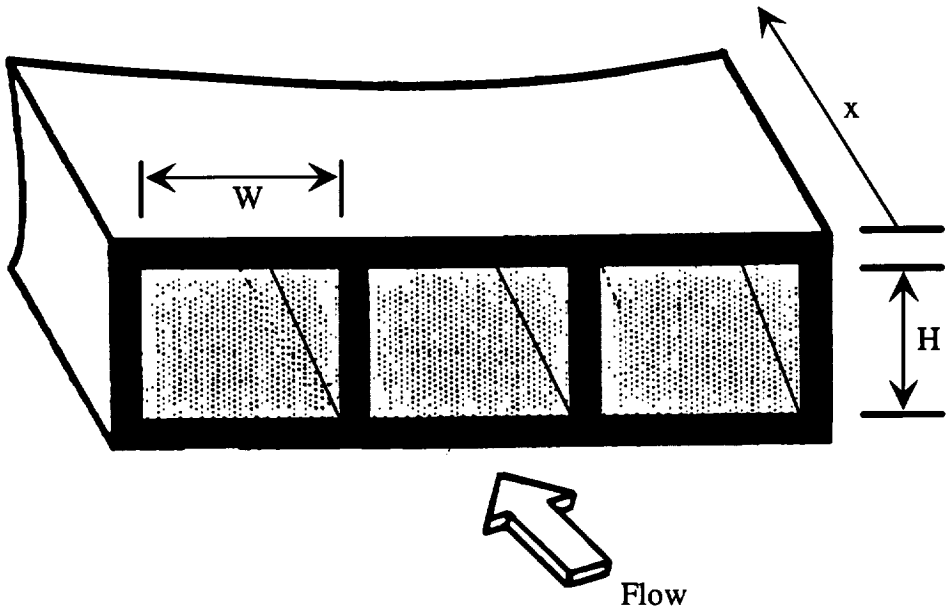

Figure 1. Straight Channel Depiction.

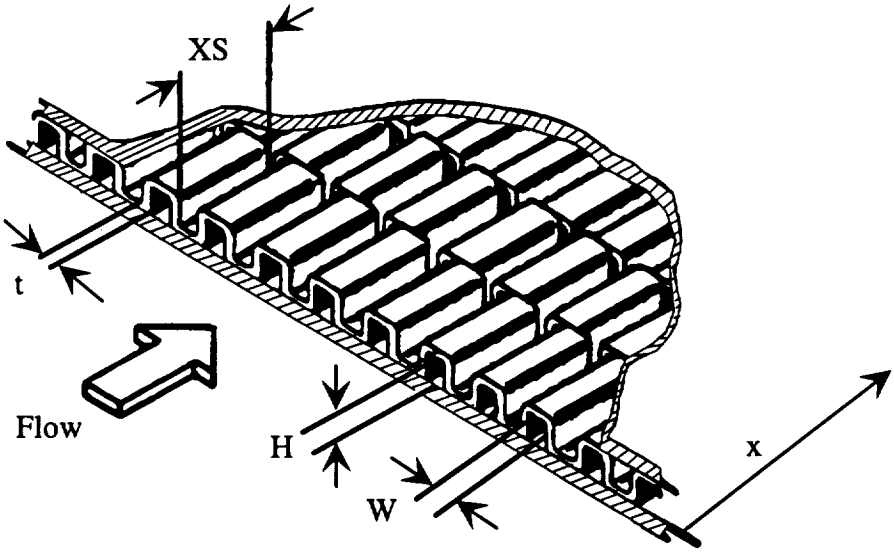

Figure 2. Offset-fin Channel Depiction (Taken from reference 7).

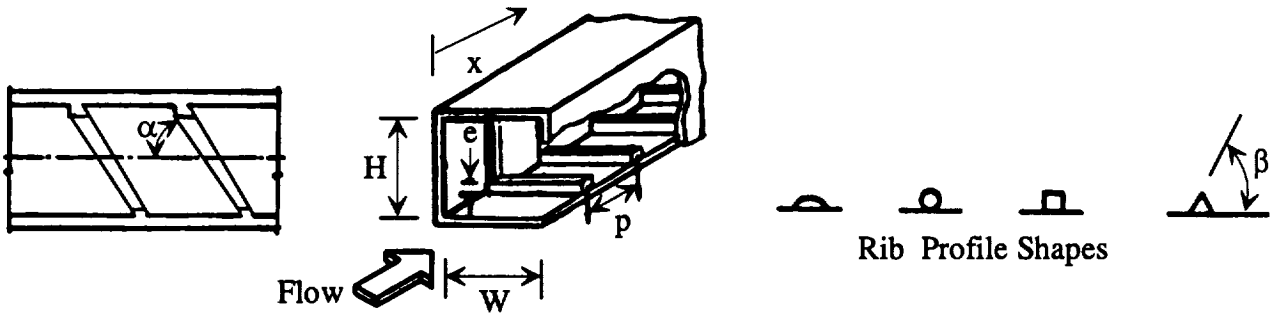

Figure 3. Ribbed Channel Depiction (Taken from reference 8).

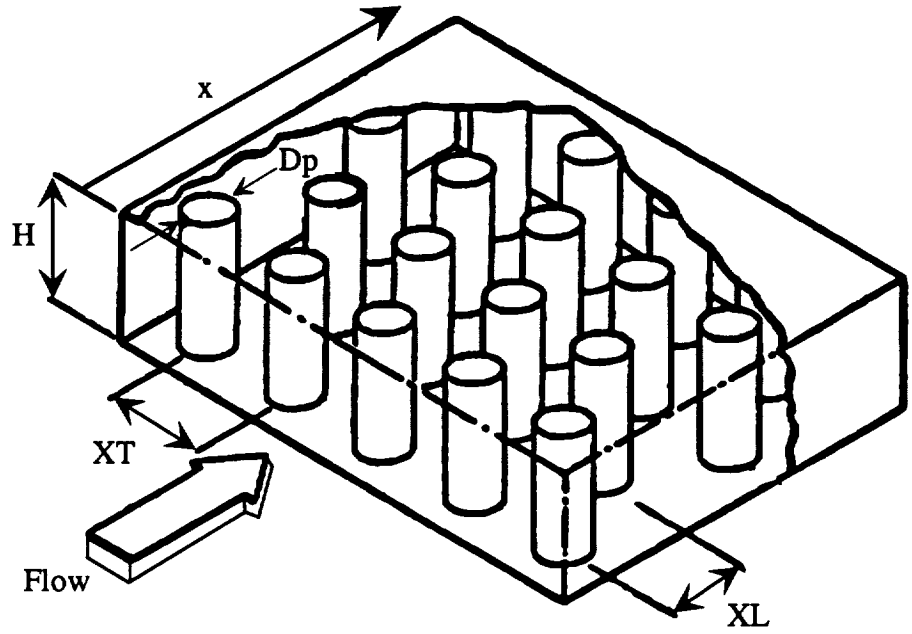

Figure 4. Pin-fin Channel Depiction (Taken from reference 14).

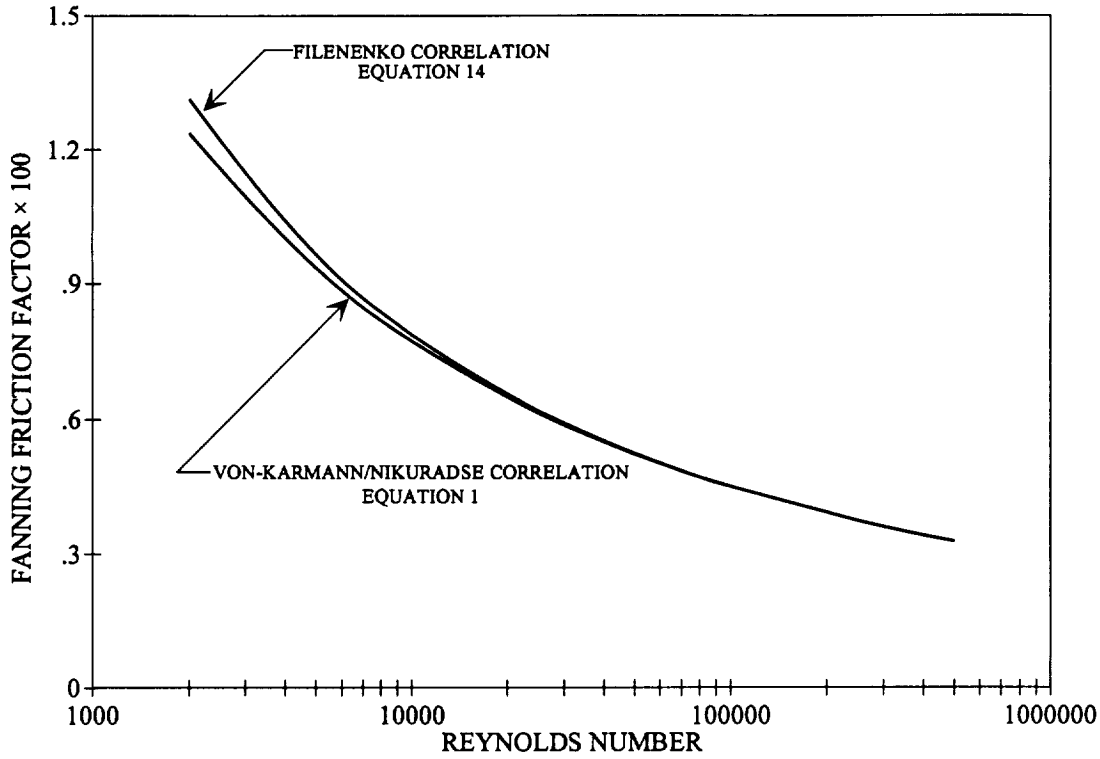

Figure 5. Smooth straight channel friction factor correlation comparison.

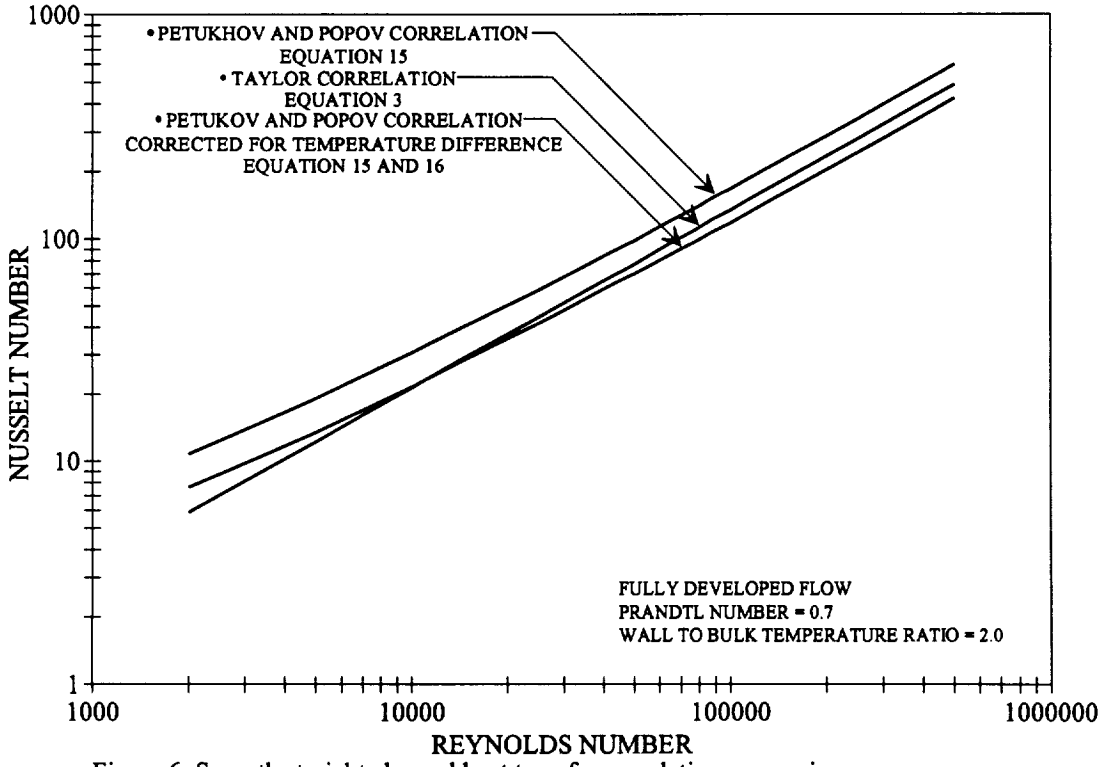

Figure 6. Smooth straight channel heat transfer correlation comparison.

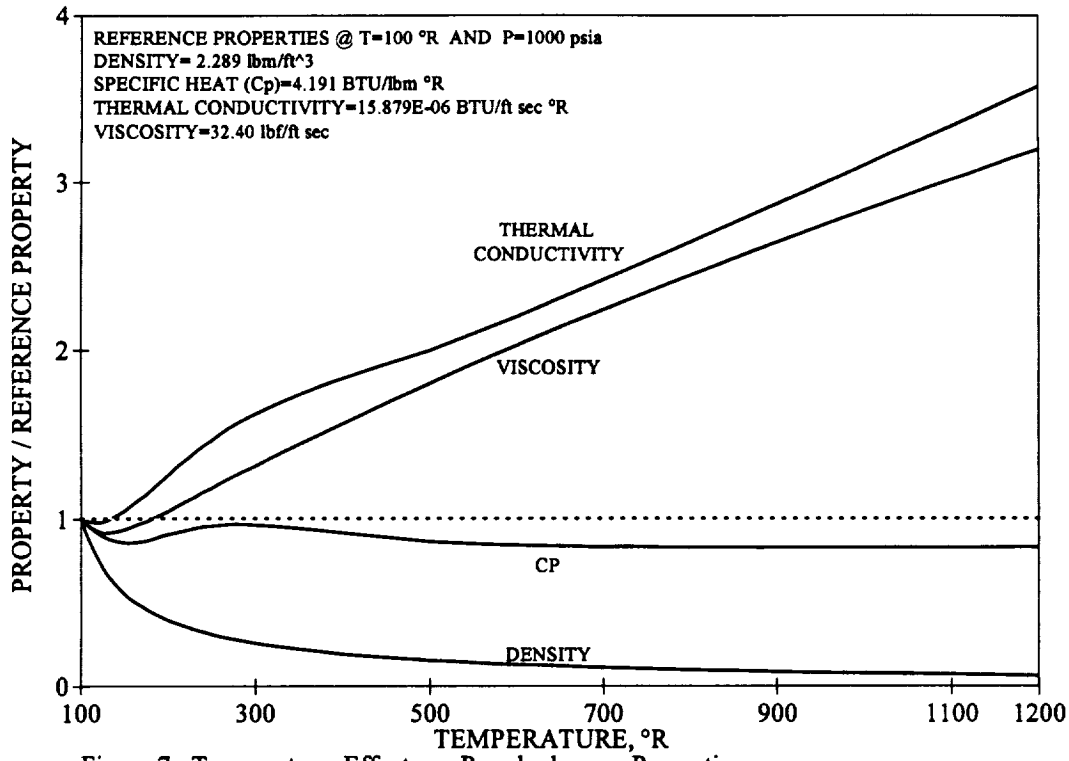

Figure 7. Temperature Effects on Para-hydrogen Properties.

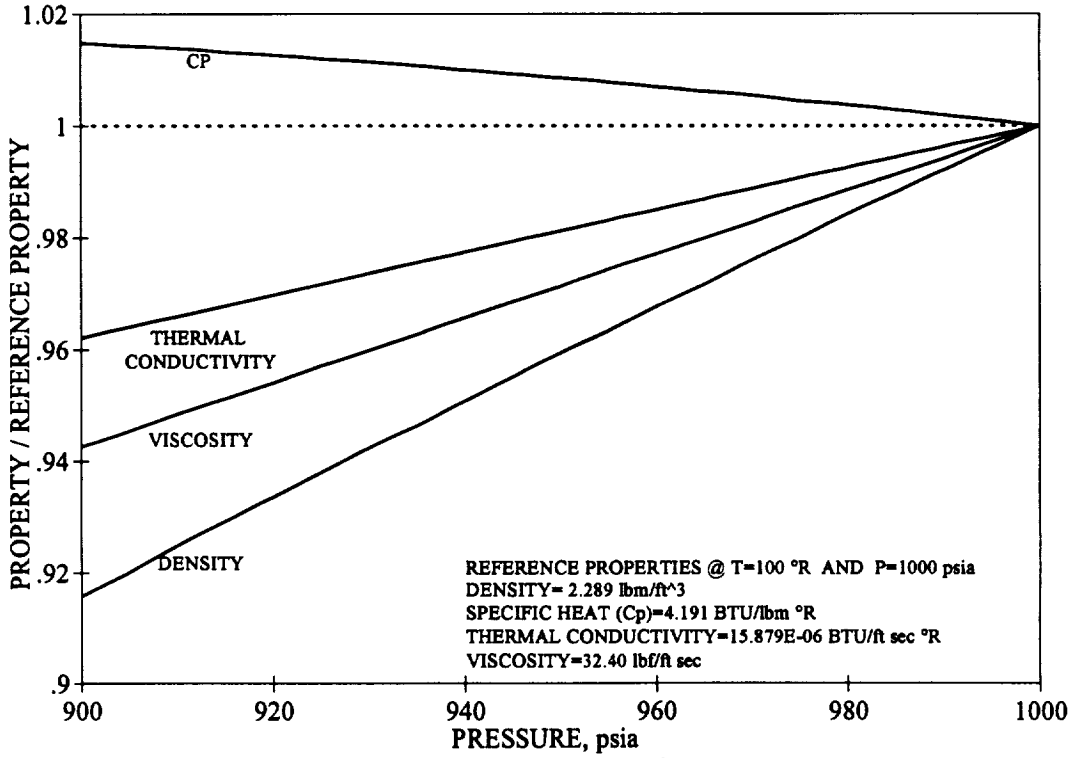

Figure 8. Pressure Effects on Para-hydrogen Properties.

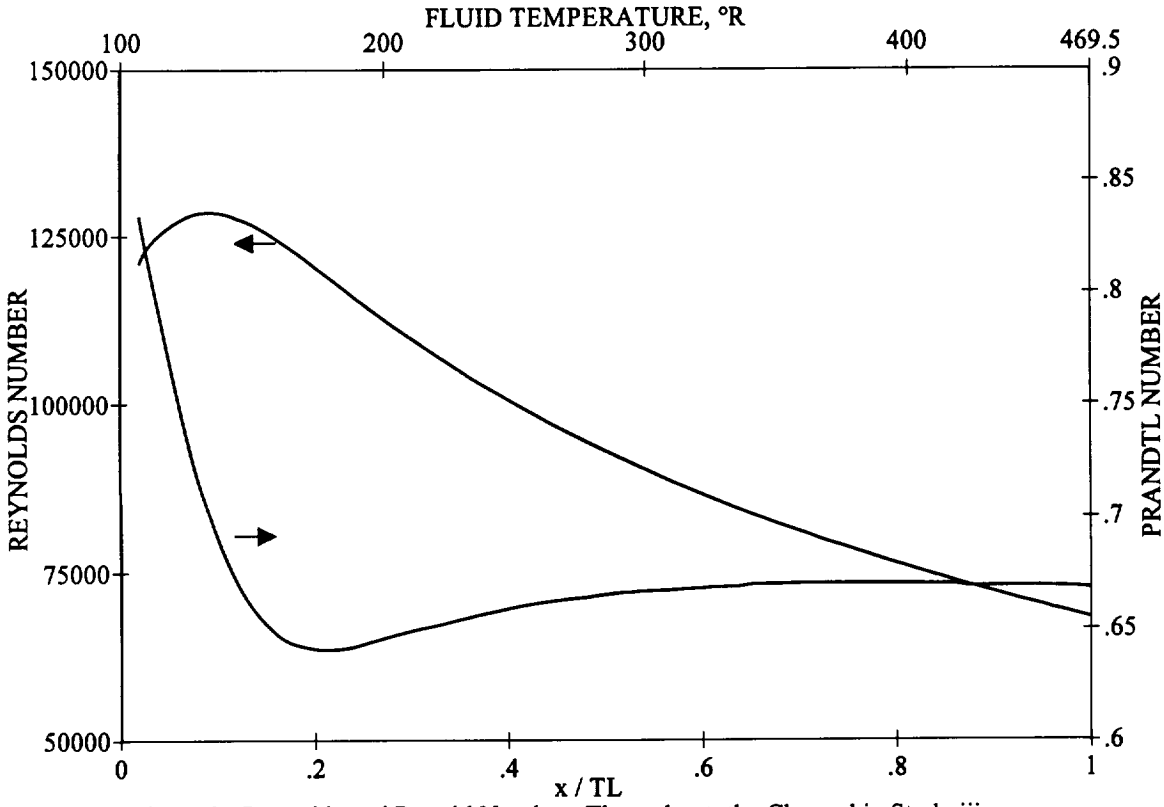

Figure 9. Reynolds and Prandtl Numbers Throughout the Channel in Study iii.

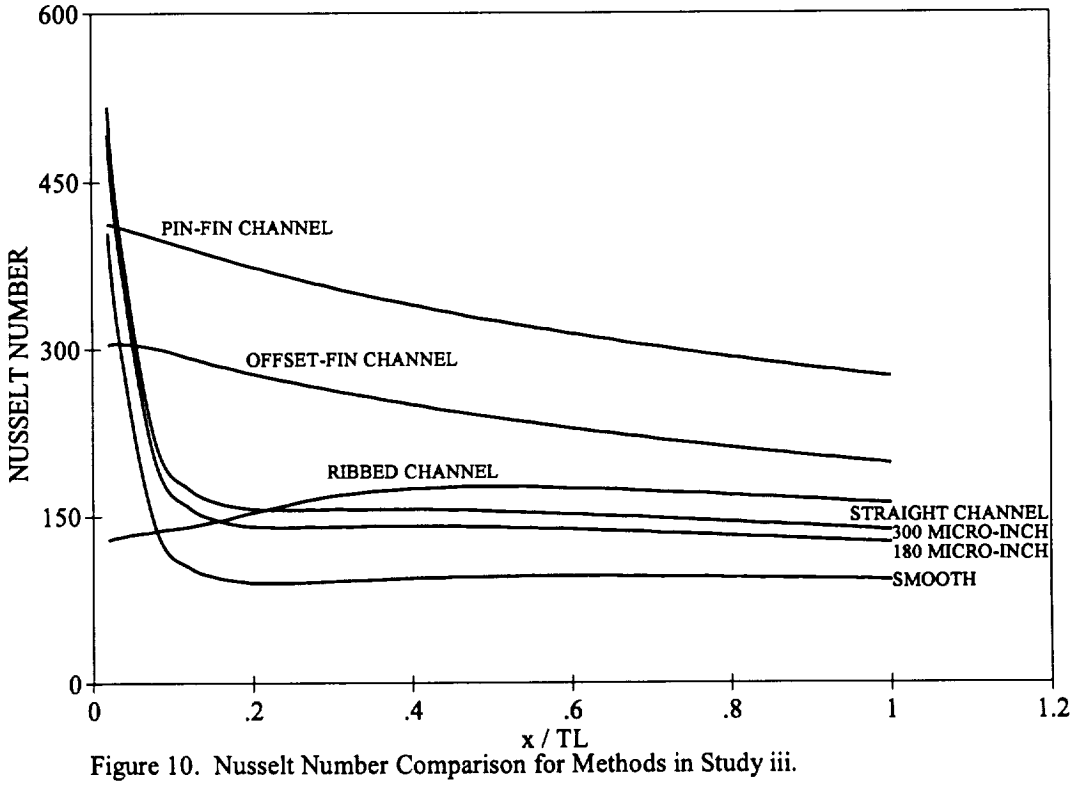

Figure 10. Nusselt Number Comparison for Methods in Study iii.

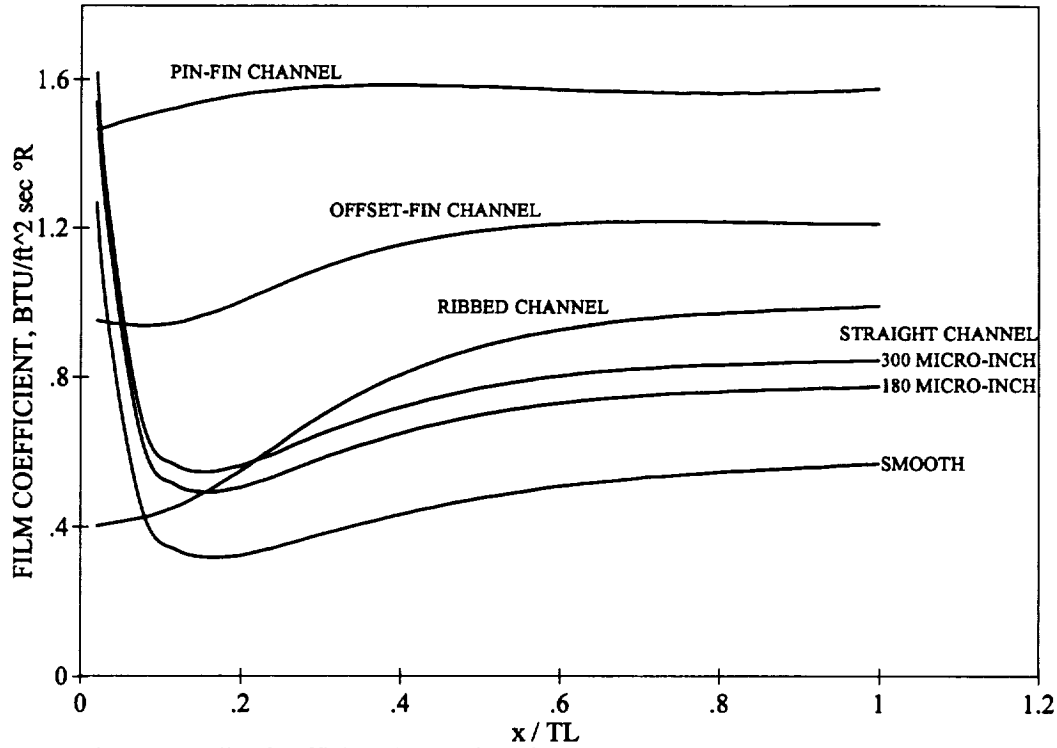

Figure 11. Film Coefficient Comparison for Methods in Study iii.

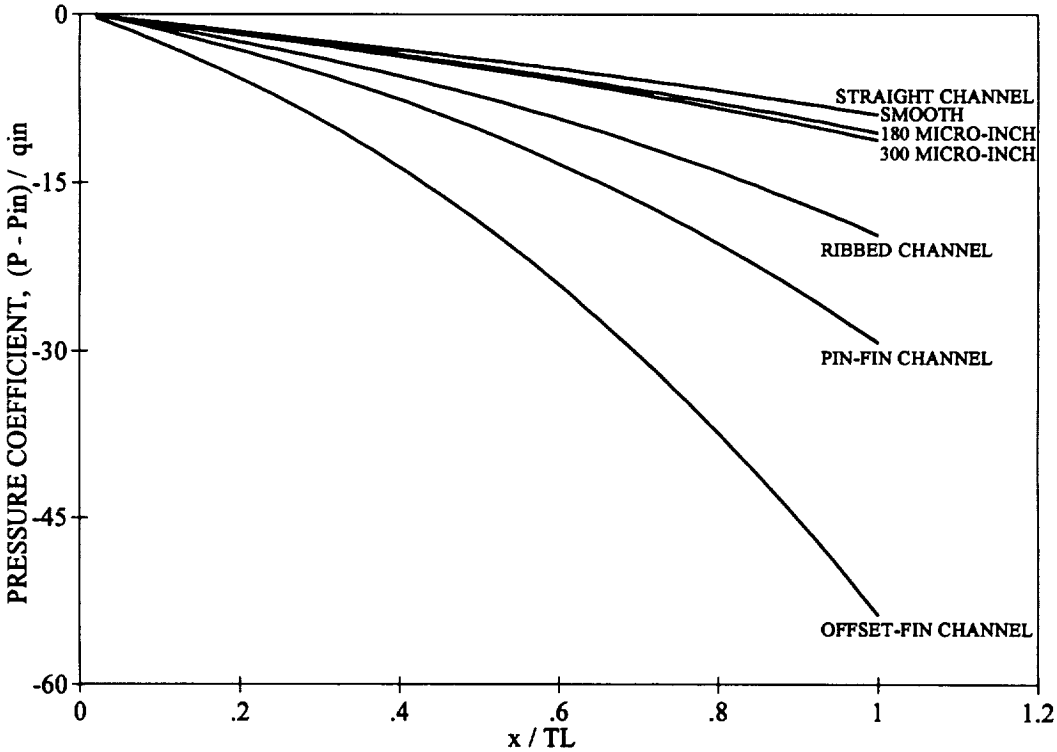

Figure 12. Pressure Coefficient Comparison for Methods in Study iii.

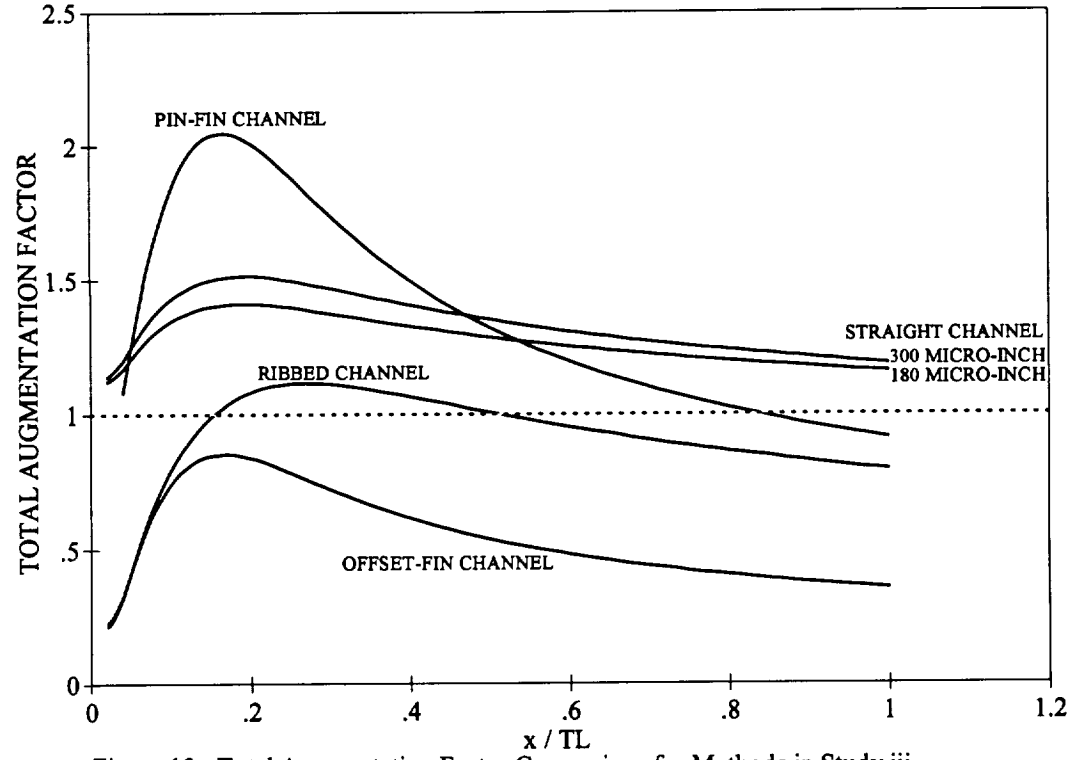

Figure 13. Total Augmentation Factor Comparison for Methods in Study iii.

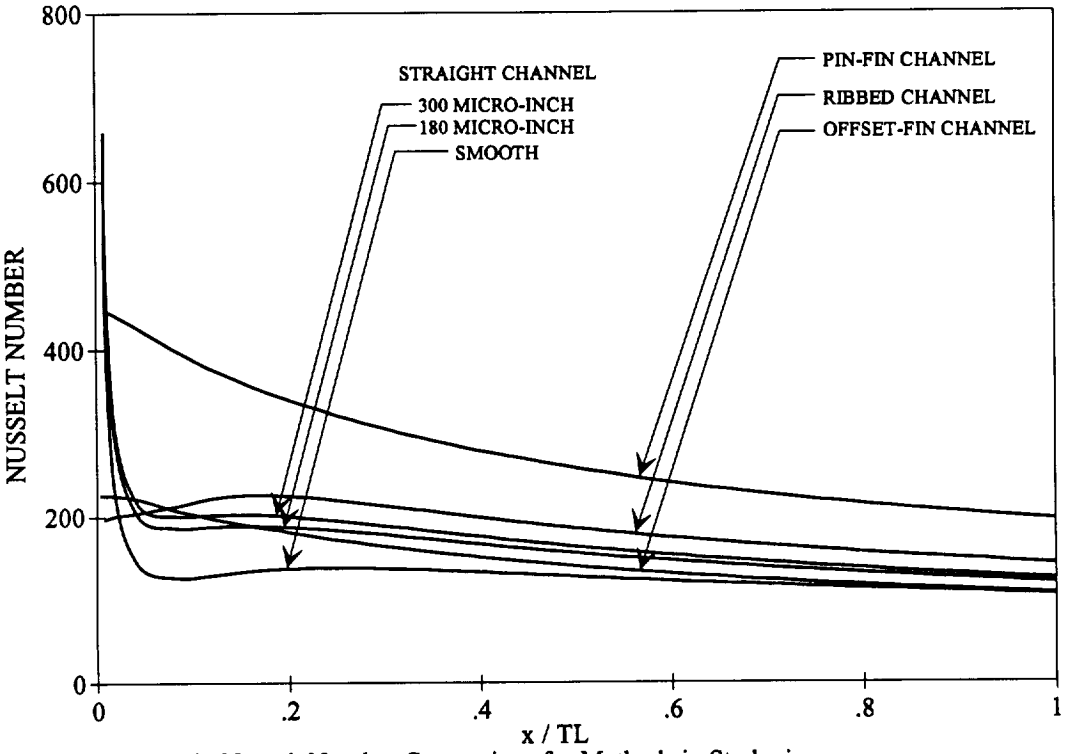

Figure 14. Nusselt Number Comparison for Methods in Study iv.

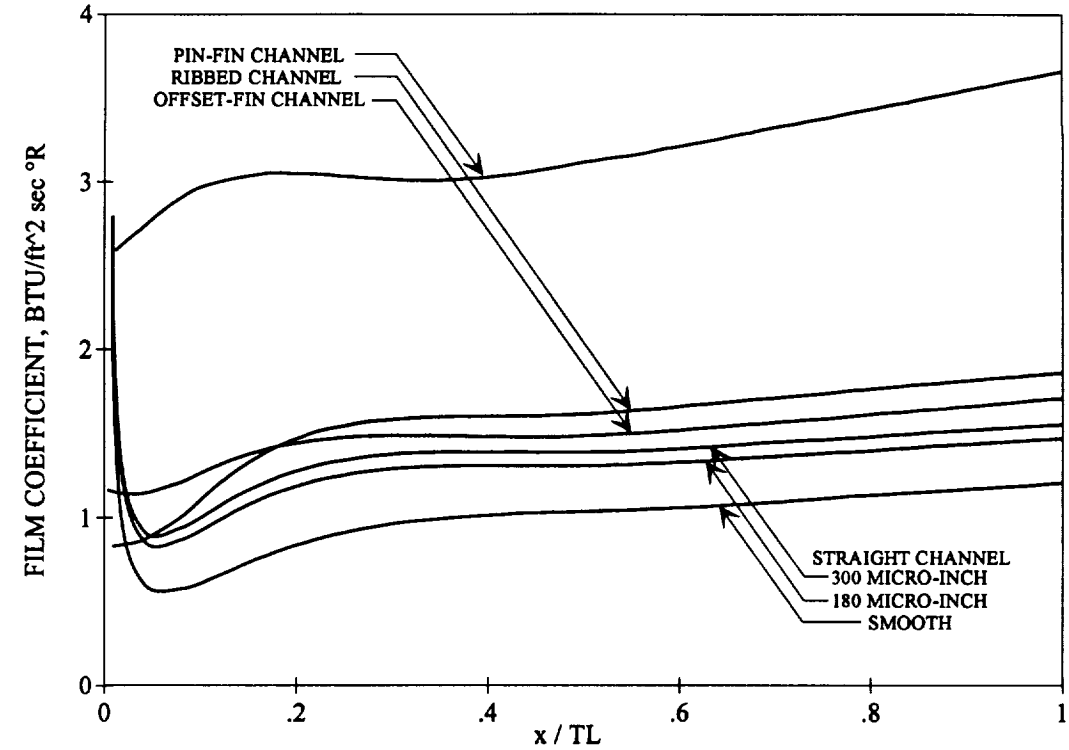

Figure 15. Film Coefficient Comparison for Methods in Study iv.

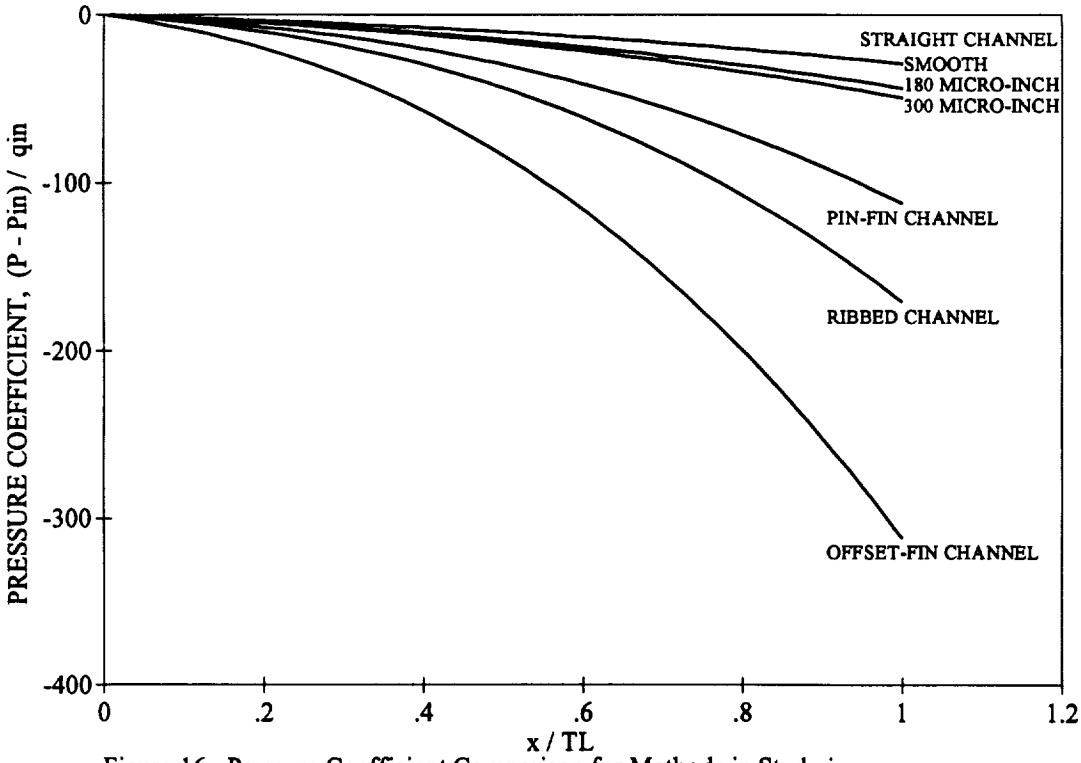

Figure 16. Pressure Coefficient Comparison for Methods in Study iv.

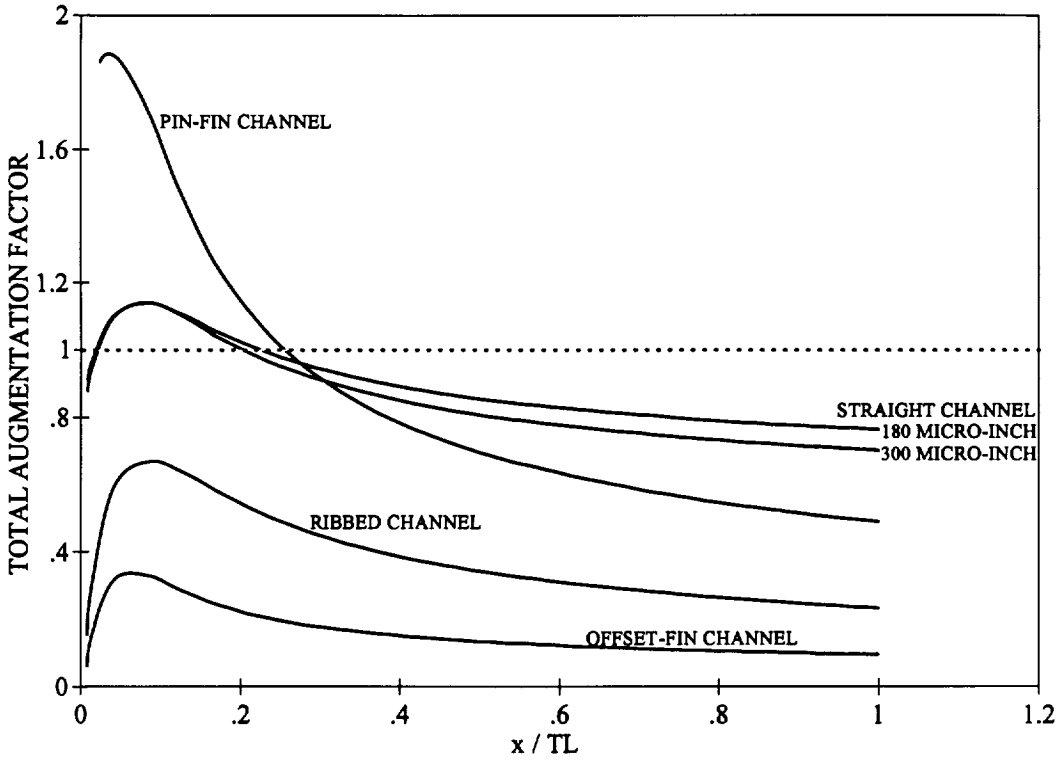

Figure 17. Total Augmentation Factor Comparison for Methods in Study iv.

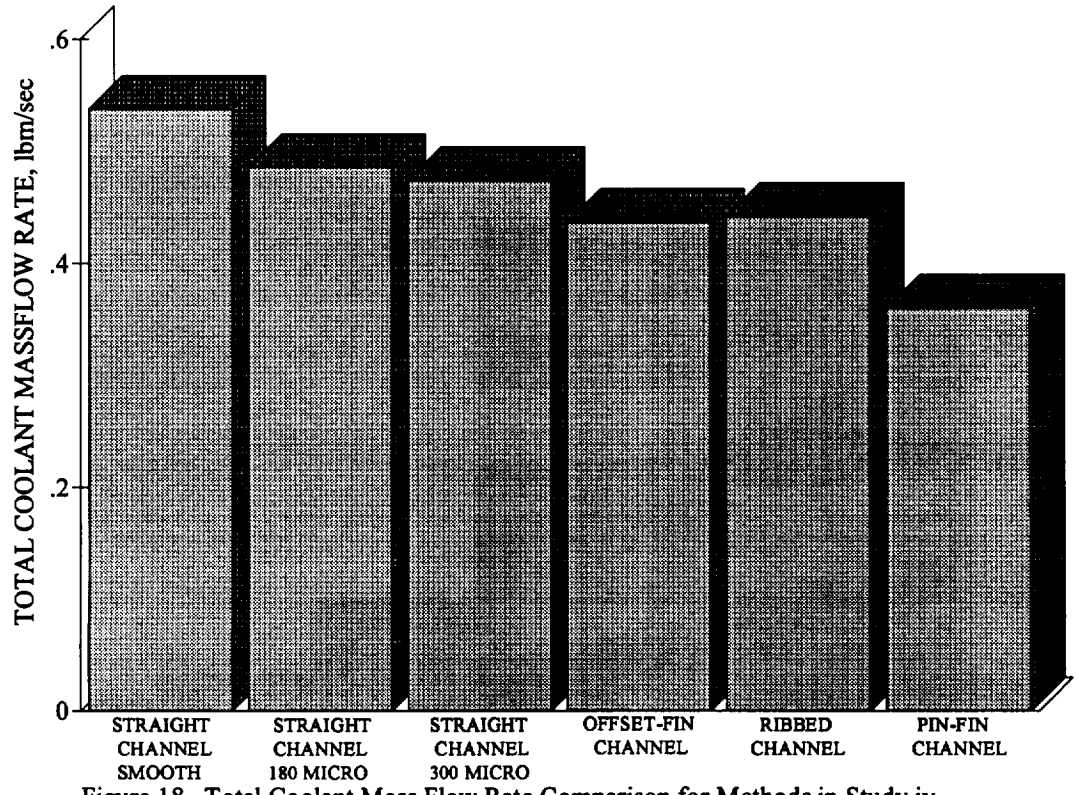

Figure 18. Total Coolant Mass Flow Rate Comparison for Methods in Study iv.

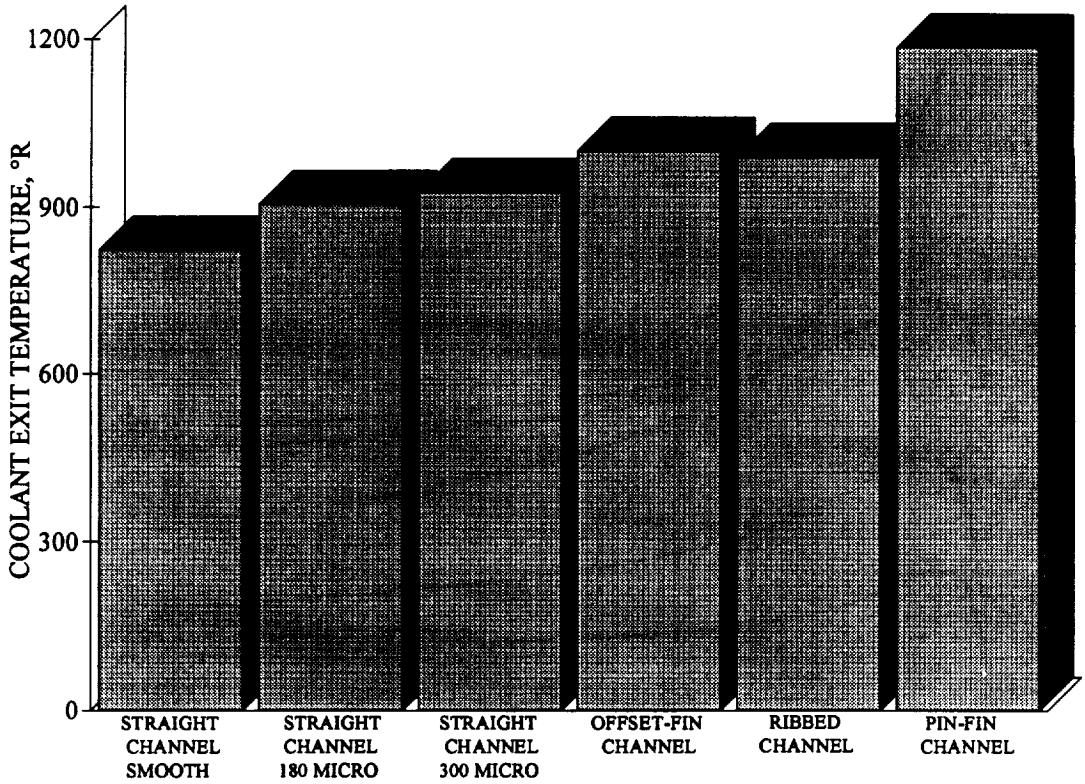

Figure 19. Coolant Exit Temperature Comparison for Methods in Study iv.

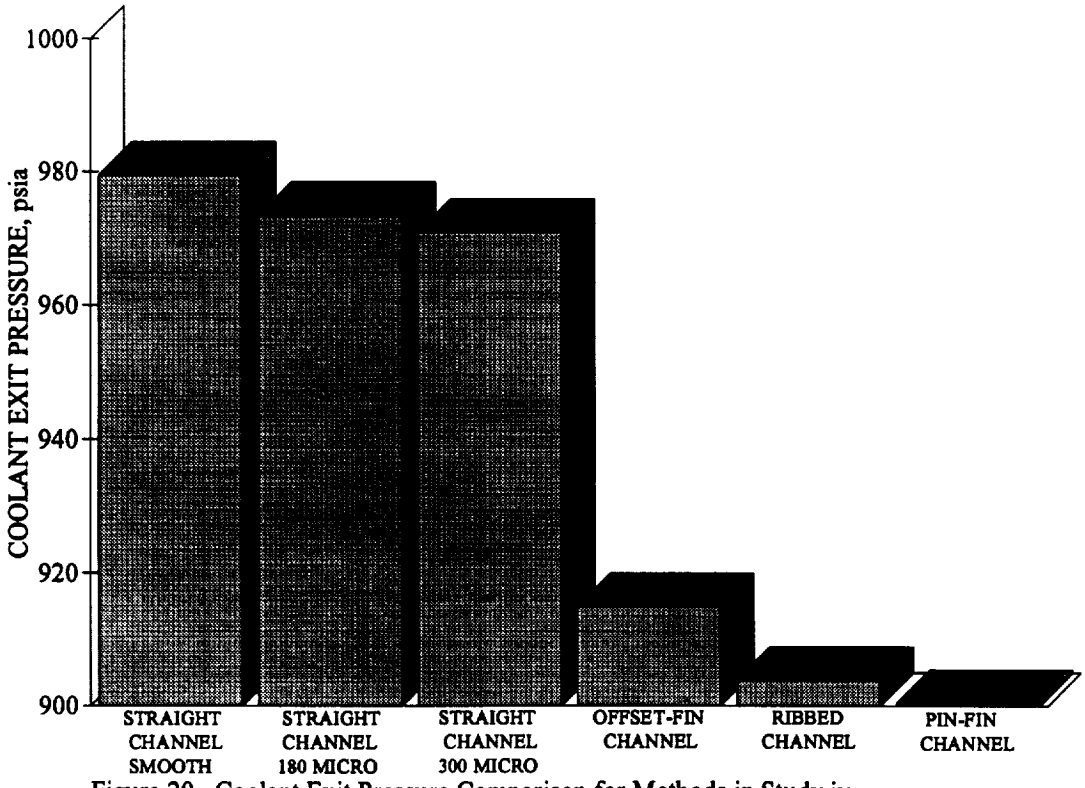

Figure 20. Coolant Exit Pressure Comparison for Methods in Study iv.

REPORT DOCUMENTATION PAGE

Form Approved
OMB No. 0704-0188

1. AGENCY USE ONLY (*Leave blank*)	2. REPORT DATE	3. REPORT TYPE AND DATES COVERED
	April 1994	Technical Memorandum

4. TITLE AND SUBTITLE

Numerical Comparison of Convective Heat Transfer Augmentation Devices Used in Cooling Channels of Hypersonic Vehicles

5. FUNDING NUMBERS

WU-505-70-69

6. AUTHOR(S)

Jaime J. Maldonado

7. PERFORMING ORGANIZATION NAME(S) AND ADDRESS(ES)

National Aeronautics and Space Administration
Lewis Research Center
Cleveland, Ohio 44135-3191

8. PERFORMING ORGANIZATION REPORT NUMBER

E-8695

9. SPONSORING/MONITORING AGENCY NAME(S) AND ADDRESS(ES)

National Aeronautics and Space Administration
Washington, D.C. 20546-0001

10. SPONSORING/MONITORING AGENCY REPORT NUMBER

NASA TM-106546

11. SUPPLEMENTARY NOTES

Responsible person, Jaime J. Maldonado, organization code 2420, (216) 433-7030.

12a. DISTRIBUTION/AVAILABILITY STATEMENT

Unclassified - Unlimited
Subject Category 34

12b. DISTRIBUTION CODE

13. ABSTRACT ***(Maximum 200 words)***

Hypersonic vehicles are exposed to extreme thermal conditions compared to subsonic aircraft; therefore, some level of thermal management is required to protect the materials used. Normally, hypersonic vehicles experience the highest temperatures in the nozzle throat, and aircraft and propulsion system leading edges. Convective heat transfer augmentation techniques can be used in the thermal management system to increase heat transfer of the cooling channels in those areas. The techniques studied in this report are pin-fin, offset-fin, ribbed and straight roughened channel. A smooth straight channel is used as the baseline for comparing the techniques. SINDA '85, a lumped parameter finite difference thermal analyzer, is used to model the channels. Subroutines are added to model the fluid flow assuming steady one-dimensional compressible flow with heat addition and friction. Correlations for convective heat transfer and friction are used in conjunction with the fluid flow analysis mentioned. As expected, the pin-fin arrangement has the highest heat transfer coefficient and the largest pressure drop. All the other devices fall in between the pin-fin and smooth straight channel. The selection of the best heat augmentation method depends on the design requirements. A good approach may be a channel using a combination of the techniques. For instance, several rows of pin-fins may be located at the region of highest heat flux, surrounded by some of the other techniques. Thus, the heat transfer coefficient is maximized at the region of highest heat flux while the pressure drop is not excessive.

14. SUBJECT TERMS

Thermal protection; Correlation; Cooling fins; Finned bodies; Fluid flow; Thermal analysis; Heat transfer correlation; Friction factor; Surface roughness

15. NUMBER OF PAGES
28

16. PRICE CODE
A03

17. SECURITY CLASSIFICATION OF REPORT	18. SECURITY CLASSIFICATION OF THIS PAGE	19. SECURITY CLASSIFICATION OF ABSTRACT	20. LIMITATION OF ABSTRACT
Unclassified	Unclassified	Unclassified	